Experimental Neurology 286 (2016) 1–11

Contents lists available at ScienceDirect

Experimental Neurology

journal homepage: www.elsevier.com/locate/yexnr

Research Paper

A new model of nerve injury in the rat reveals a role of Regulator of G protein Signaling 4 in tactile hypersensitivity

Giuliano Taccola [a,b,c,1], Pierre J Doyen [a,1], Jonathan Damblon [a], Nejada Dingu [a,b,c], Beatrice Ballarin [a], Arnaud Steyaert [a], Anne des Rieux [d], Patrice Forget [a], Emmanuel Hermans [a], Barbara Bosier [a], Ronald Deumens [a,*]

[a] Institute of Neuroscience, Université catholique de Louvain, Av. Hippocrate 54, Brussels, Belgium
[b] Neuroscience Department, International School for Advanced Studies (SISSA), via Bonomea 265, Trieste, TS, Italy
[c] SPINAL (Spinal Person Injury Neurorehabilitation Applied Laboratory), Istituto di Medicina Fisica e Riabilitazione (IMFR), via Gervasutta 48, Udine (UD), Italy
[d] Louvain Drug Research Institute, Av. Mounier 73, Brussels and Institute of Condensed Matter and Nanosciences, Université catholique de Louvain, 1348 Louvain-la-Neuve, Belgium

ARTICLE INFO

Article history:
Received 29 July 2016
Received in revised form 13 September 2016
Accepted 14 September 2016
Available online 15 September 2016

Keywords:
Neuropathic pain
Animal model
Allodynia
Chronification
RGS
Glia

ABSTRACT

Tactile hypersensitivity is one of the most debilitating symptoms of neuropathic pain syndromes. Clinical studies have suggested that its presence at early postoperative stages may predict chronic (neuropathic) pain after surgery. Currently available animal models are typically associated with consistent tactile hypersensitivity and are therefore limited to distinguish between mechanisms that underlie tactile hypersensitivity as opposed to mechanisms that protect against it. In this study we have modified the rat model of spared nerve injury, restricting the surgical lesion to a single peripheral branch of the sciatic nerve. This modification reduced the prevalence of tactile hypersensitivity from nearly 100% to approximately 50%. With this model, we here also demonstrated that the Regulator of G protein Signaling 4 (RGS4) was specifically up-regulated in the lumbar dorsal root ganglia and dorsal horn of rats developing tactile hypersensitivity. Intrathecal delivery of the RGS4 inhibitor CCG63802 was found to reverse tactile hypersensitivity for a 1 h period. Moreover, tactile hypersensitivity after modified spared nerve injury was most frequently persistent for at least four weeks and associated with higher reactivity of glial cells in the lumbar dorsal horn. Based on these data we suggest that this new animal model of nerve injury represents an asset in understanding divergent neuropathic pain outcomes, so far unravelling a role of RGS4 in tactile hypersensitivity. Whether this model also holds promise in the study of the transition from acute to chronic pain will have to be seen in future investigations.

1. Introduction

The search for the cellular and/or molecular underpinnings of persistent pain states has intensified over the past decades. The advances in our mechanistic understanding of chronic pain, which affects 30–50% of the general population (Bouhassira et al., 2008; Torrance et al., 2006) are heavily based on animal models of peripheral nerve injury (Gregory et al., 2013). Chronic pain often has neuropathic characteristics (Lavand'homme, 2011) and, as chronic pain, neuropathic pain is highly intractable (Baron et al., 2010). Nevertheless, nerve lesions do not always lead to persistent pain as illustrated by half the surgical amputees who do not develop chronic postoperative pain (Kehlet et al., 2006). We still know only little about the factors that facilitate versus the factors that protect against a transition from acute to chronic pain (Deumens et al., 2013).

Longitudinal studies on postoperative patients show a 10–50% prevalence of chronic pain, strongly associated with nerve lesions (Kehlet et al., 2006). Clinical data suggest that tactile hypersensitivity early after surgery holds predictive value for chronic (neuropathic) postoperative pain (Lavand'homme et al., 2005; Martinez et al., 2012). While tactile hypersensitivity does not consistently develop after surgery or nerve injury in human, most animal models of peripheral nerve injury show consistent tactile hypersensitivity (Gregory et al., 2013). Interestingly, the prevalence of tactile hypersensitivity after injury to the rat spinal cord was found to depend on the extent of tissue trauma (Kloos et al., 2005). This made us wonder whether restricting the extent of tissue

Abbreviations: CB_1 receptor, cannabinoid type-1 receptor; DRG, dorsal root ganglion; GFAP, glial fibrillary acidic protein; Iba1, ionized calcium-binding adapter molecule 1; MPE, maximum-possible-effect; mSNI, modified spared nerve injury; PWT, paw withdrawal threshold; RGS4, Regulator of G protein Signaling 4; SNI, spared nerve injury; SSI, static sciatic index.

* Corresponding author at: Institute of Neuroscience, Université catholique de Louvain, Av. Hippocrate 54, Brussels, Belgium.
E-mail addresses: ronald.deumens@uclouvain.be, deumensr@gmail.com (R. Deumens).

[1] Authors contributed equally to the manuscript.

http://dx.doi.org/10.1016/j.expneurol.2016.09.008
0014-4886/

trauma after peripheral nerve injury could reduce the prevalence of tactile hypersensitivity as well.

The prevalence of neuropathic pain-like behaviours such as tactile hypersensitivity may also depend on the choice of rat strain (Yoon et al., 1999). Nearly 50% of Holtzman rats were found to be protected against tactile hypersensitivity through an engagement of inhibitory projections descending from the brainstem to the spinal cord and modulating local nociceptive networks in the dorsal horn (De Felice et al., 2011). The failure to engage such inhibitory systems in the other 50% of rats remains largely unexplained, but disinhibition within the nociceptive system has been repeatedly documented after nerve injury, at multiple locations of the neuraxis (Blom et al., 2014; von Hehn et al., 2012).

A multitude of neuropathic mechanisms may cause disinhibitory states in the central nervous system (CNS), both of neuronal and non-neuronal (immune) origin. We recently demonstrated that the signaling efficacy of the analgesic cannabinoid type-1 (CB_1) receptors was reduced in the spinal cord of nerve injured rats due to an injury-induced up-regulation in Regulator of G protein Signaling 4 (RGS4) (Bosier et al., 2015). RGS is a family of multifunctional proteins that promote the termination of signaling through G protein-coupled receptors, and previous work already linked spinal RGS4 with a loss of opioid receptor signaling efficacy after peripheral nerve injury in the rat (Garnier et al., 2003).

In the present study, we modified the model of spared nerve injury in the rat in order to limit the extent of tissue trauma. Tactile hypersensitivity, which occurred in only 50% of rats with modified spared nerve injury, was found to be associated with an increased expression of RGS4.

2. Materials and methods

2.1. Animals: models of peripheral nerve injury

A total of 149 adult female Sprague Dawley rats, 10–12 weeks old, were used, 139 under ethical approval of the Belgium authority on animal experimentation (LA2230419) and 10 under ethical approval of the Italian authority on animal experimentation (the Scuola Internazionale Superiore di Studi Avanzati (SISSA) ethics committee). All experiments were conducted under strict regulations, respecting the European Community Council directive of 24 November 1986 (86–609/ECC) and the decree of 20 October 1987 (87–848/EEC). The animals were kept in groups of 2–3 animals per standard makrolon cage with ad libitum access to food at a regular 12:12 h light-dark cycle. An exception to this rule of social housing applied to animals receiving an indwelling intrathecal catheter, i.e. a total of n = 24 rats that were individually housed. Animals were either subjected to nerve injury (n = 124) or sham-surgery (n = 15) using methods reported previously (Decosterd and Woolf, 2000), but with slight modifications. In brief, the sciatic nerve was exposed *at random* on either the left or the right side under sevoflurane anaesthesia (6% in oxygen for induction; 2–3% in oxygen for maintenance) and aseptic conditions. Then, the three peripheral nerve branches of the sciatic nerve (i.e. tibial, common peroneal and sural nerve branches) were exposed through blunt dissection and freed from the surrounding connective tissue. Animals were *ad random* divided into three groups: (1) spared nerve injury (SNI; n = 21), (2) modified SNI (mSNI; n = 103), and (3) sham surgery (n = 15). For SNI, the tibial and common peroneal nerve branches were injured while for mSNI only the common peroneal nerve branch was injured. Injury was inflicted using a non-serrated nerve clamp, i.e. the De Beer clamp (Honer Medizin-Technik GmbH & Co., Spaichingen, Germany) exerting a force of 54 N over a period of 30 s (Luis et al., 2007). In both mSNI and SNI the sural nerve branch was left intact (spared). Sham surgery involved skin incision and the sciatic nerve branches were dissected free, but were not crushed. Then, wounds were closed using 4/0 prolene sutures and animals were returned to their home cage. Postoperative care did not include pain medication as this might interfere with the primary study outcome, i.e. the development of neuropathic pain-like behaviour.

2.2. Electrophysiology

Adult female rats were anaesthetized with CO_2 and then sacrificed through CO_2 asphyxiation followed by cervical dislocation in line with the guidelines provided by the Italian Animal Welfare act, following the European Directive for animal experiments 2010/63/EU. Sciatic nerves were carefully dissected out from dorsal vertebrae to the ankle. One sciatic nerve per animal was used and each time the side (right or left leg) was randomly selected (n = 10 animals; 5 right, 5 left). At the end of the experiment, a precision caliper was used to carefully measure the mean lengths of the three peripheral branches of the sciatic nerve (tibial branch = 40.85 ± 2.31 mm; common peroneal branch 34.60 ± 2.15 mm; sural branch = 28.62 ± 2.942 mm (n = 10)).

As for electrophysiological recordings, monopolar glass suction electrodes were used to draw in the peripheral extremity of each branch, while stimuli were delivered to the sciatic nerve using a concentric bipolar electrode (see cartoon in Fig. 1A). Signals were recorded in AC, amplified 1000 times (DP-304®, Warner Instruments, CT), digitalized (250 KHz, Digidata® 1440 A, Molecular Devices Corporation, CA) and stored in a personal computer for further analysis. Single pulses (total width = 0.2 ms) were delivered as cathodic-first charge-balanced biphasic rectangular current injections without a delay between cathodal and anodal phases. In order to obtain input/output curves, we delivered a train of stimuli (0.33 Hz) of increasing amplitude (80 stimuli, 5 pulses for each steps from 10 to 160 μA). The stimulating threshold was defined as the minimum pulse strength able to evoke an appreciable response (for tibial = 20.00 ± 1.67 μA; common peroneal = 23.33 ± 1.67 μA; sural = 23.33 ± 1.67 μA; n = 10). Nerve injury was inflicted onto both tibial and common peroneal branches (see cartoon in Fig. 1B) as described earlier. In order to prevent decay of signal amplitude with the slightest movements of nerve extremities during clamp manipulation, we released all suctions after control recordings. After lesion, the nerve clamp was removed and new suctions were performed with the same glass electrodes, to obtain an identical seal as in control conditions. The same procedures were performed on the unlesioned (spared) sural nerve, which served as an internal control. Time to peak was calculated as the time spanning from the first stimulation artifact to the peak of response. At least five traces were averaged for each stimulation intensity. Conduction velocity was expressed in m/s and resulted from a division of fiber length by the mean time to peak for the maximal stimulation strength applied (160 μA).

2.3. Algesimetry

After habituating the animals to the experimenter (R.D.), the animals were placed in transparent plastic chambers without floor, positioned on an elevated wire mesh. Acclimatization was allowed for a period of about 20 min after which the von Frey test was performed. Herein, a set of eight calibrated von Frey hair filaments (Stoelting, Wood Dale, IL, US) was used (0.4, 0.7, 1.2, 2.0, 3.6, 5.5, 8.5, 15.1 g). Filaments were applied to the plantar hind paw surface and held in a slightly buckled position for a period of around 8 s, starting with the 2 g-filament. The choice for the following filament was based on the response to the previous filament application, being the closest-lower filament in case of a positive withdrawal response ('x') or the closest-higher filament in case of a negative withdrawal response ('o'). A positive withdrawal response was defined by a paw withdrawal associated with aversive behaviour, such as keeping the stimulated paw elevated, licking the paw, or attacking or biting of the filament. This method of filament application was continued until a sequence of six filament applications was acquired starting either with 'o-x' or with 'x'. In case the upper-end filament (15.1 g) or the lower-end filament (0.4 g) was

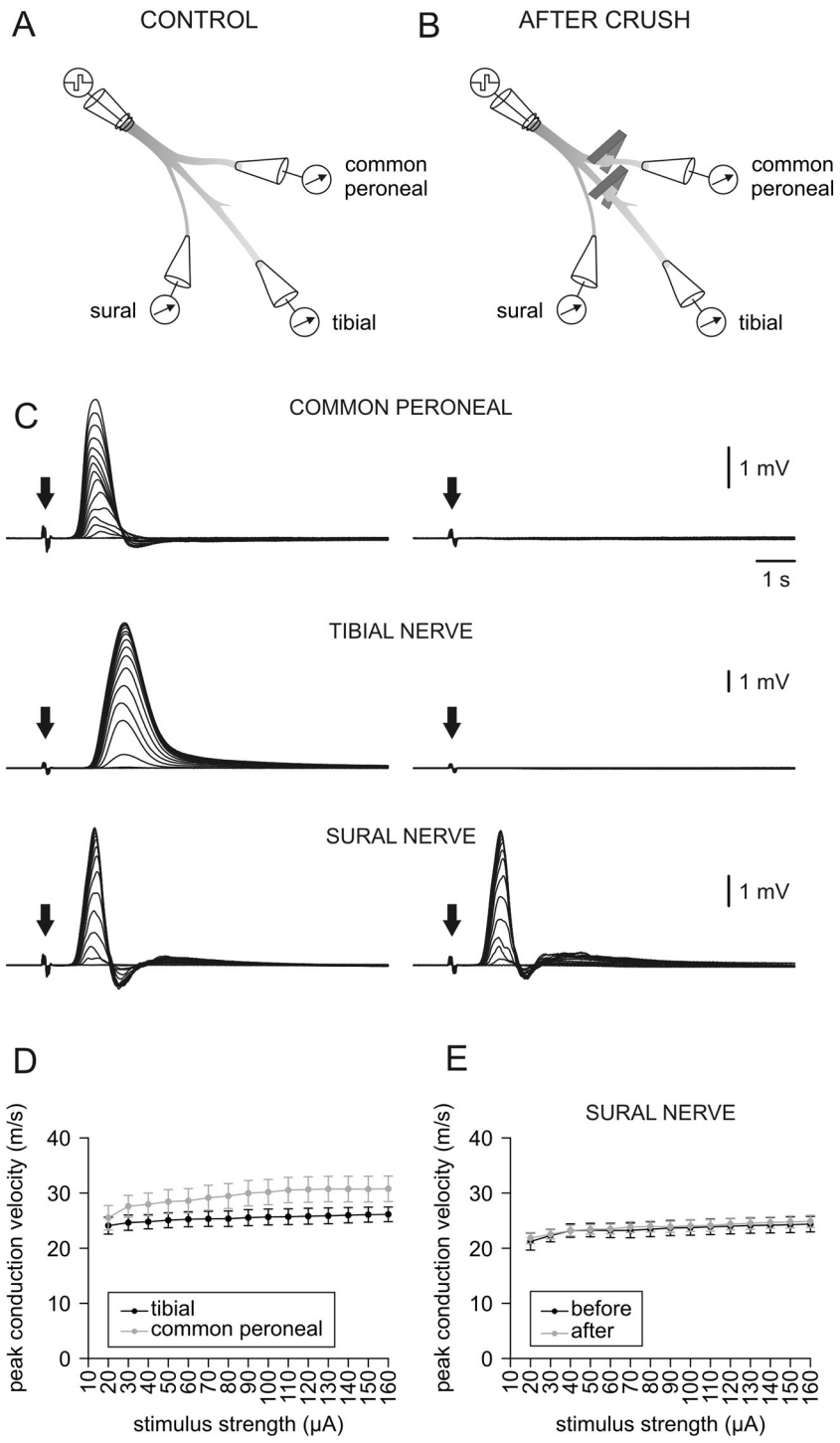

Fig. 1. Functional (electrophysiological) responses measured before and after crush injury. A; cartoon depicting the setting for electrophysiological experiments. A stimulating suction electrode was positioned at the proximal end of an isolated sciatic nerve while three suction electrodes recorded responses from the three peripheral ends of the sciatic nerve. B; sites of standardized crush are shown as sketched clamp positions. Traces in C result from input/output experiments performed in control (left) conditions and after lesion of the common peroneal and tibial branches (right). Note that injured branches were completely silenced while the unlesioned (spared) sural branch retains responses comparable to control. Arrows indicate stimulation artefacts; the different time to peak for the three responses corresponds to minimal differences in length of the three branches that, indeed, still maintained comparable conduction velocities. D; conduction velocities in control conditions for tibial (black) and common peroneal (grey) at increasing pulse strengths (n = 10). E; conduction velocities of the spared sural nerve before and after crush procedures (n = 10). Note superimposed dots before and after lesion indicating that sural responses were not affected by clamping procedures.

reached, no more filaments were applied any further. The 50% paw withdrawal threshold (PWT) was then calculated as described previously (Chaplan et al., 1994). In case of merely positive or merely negative responses to any filament, cut-off values were assigned (0.4 g and 15.1 g, respectively). Only the sural nerve territory at the glabrous plantar hind paw surface was stimulated throughout the experiment as this territory remained innervated in both injury models (SNI and mSNI), thus allowing for the assessment of stimulus-response behaviours. In order to determine on an individual level whether animals developed tactile hypersensitivity, we considered PWT-changes used in the literature to confirm efficacy of pain-treatments (Smits et al., 2006), i.e. a change of 50% in the PWT (in grams).

2.4. Static sciatic index

A subset of animals (n = 15) was used to monitor the static sciatic index (SSI) as a read-out of a sciatic nerve-dependent motor function. Briefly, rats were placed on a plastic surface in a plastic box and a webcam (Logitech HD webcam) positioned underneath the set-up was connected to a personal computer. Before and at multiple time points (until three weeks) after mSNI surgery a total of minimally 5 photographs were taken when animals were showing normal stance (non-rearing; all four paws in contact with the floor). SSI scores were calculated as described previously (Bervar, 2000). Briefly, the photomicrographs were loaded into NIH ImageJ software (version 1.45k) and four measures were taken: the outer toe spread (TS) of both the ipsilateral and contralateral hindpaws (distance between toes 1 and 5) and the inner toe spread (ITS) of both the ipsilateral and contralateral hindpaws (distance between toes 2 and 4). Then, the toe spread factor (TSF) as well as the intermediate toe spread factor (ITSF) were calculated: TSF = (ipsilateral TS – contralateral TS)/contralateral TS; ITSF: (ipsilateral ITS – contralateral ITS)/contralateral ITS. Finally, the SSI score was calculated per the following formula: SSI = (108.44 × TSF) + (31.85 × ITSF) – 5.49. Animals were finally divided into mSNI+ and mSNI− groups based on the 7-day PWT and respecting the 50% change in PWT as described earlier.

2.5. qRT-PCR

A subset of 17 rats was used for qRT-PCR analyses. The ipsilateral and contralateral lumbar (L4 and L5) DRGs and the ipsilateral and contralateral dorsal lumbar spinal cord were dissected one week after sham-surgery (n = 4), mSNI+ (n = 5) and mSNI− (n = 8). Total RNA was isolated using TriPure isolation reagent (Roche Diagnostics, Vilvoorde, Belgium), treated with the RQ1 RNase-free DNase kit (Promega, Leiden, Netherlands) and reverse transcribed with the iScript cDNA synthesis kit (Bio-Rad Laboratories, Nazareth, Belgium). Real-time PCR amplifications were carried out using the iCycler IQ™ multicolour real time PCR detection system (Bio-Rad Laboratories, Nazareth, Belgium), in a total volume of 25 μl containing 10 ng cDNA template, 0.3 μM of the primers (see hereafter) and the IQ™ SYBR Green Supermix using an annealing temperature of 60 °C. For quantitative analysis, a relative standard curve was generate using the same amplification conditions and with dilutions of a mix of cDNA templates (from 20 to 0.078 ng). Each sample was normalized to the relative amplification of glyceraldehyde 3-phosphate dehydrogenase (GAPDH) as a housekeeper gene. Relative quantification of mRNA in the samples was performed using the post-run data analysis software provided with the iCycler system. The following primer sequences were used; RGS4 forward primer: 5′ taacttgccagagggtgagc3′, reverse primer: 5′aaagctgccagtccacattc3′; RGS2 forward primer: 5′agcaaatatgggcttgctgcat3′, reverse primer: 5′ gcctcttggatattttgggcaatc3′; GAPDH forward primer: 5′gtctcctgtg acttcaacag3′, reverse primer: 5′agttgtcattgagagcaatgc3′.

2.6. RGS4 inhibitor experiment

A subset of animals (n = 24) received an indwelling intrathecal catheter, which was implanted immediately prior to mSNI. Under the same (sevoflurane) anaesthesia as described before, the atlanto-occipital membrane was freed and a slit was made through the underlying dura mater. The catheter was advanced into the intrathecal space up to 8.5 cm in order to have the catheter reach the lumbar enlargement. Prior to any further experimentation on day 7, 10 μl of 2% lidocaine was injected into the intrathecal catheter, followed by a 20 μl saline flush. All animals displayed a transient paresis of the hindpaws after this procedure, confirming the correct positioning of the catheter. Hereafter, algesimetric analysis was performed to distinguish between mSNI animals with and without tactile hypersensitivity. Out of the 24 animals, 11 showed tactile hypersensitivity and were used for further experimentation. Six of the latter animals received 0.5 μg CCG63802 (a specific RGS4 inhibitor; Tocris, cat. no. 4028, Bristol, UK; concentration of 0.05 mg/ml dissolved in 5% DMSO in saline) in a total volume of 10 μl, administered through the intrathecal catheter, as previously described (Bosier et al., 2015). The remaining five animals received 10 μl of vehicle solution (5% DMSO in saline). A 20 μl saline flush immediately followed the intrathecal injection of either CCG63802 or vehicle. Hereafter, algesimetric analysis was performed every 20 min for a total duration of 2 h. The results on PWT were then expressed as the maximum-possible-effect (MPE), calculated as follows: (posttreatment individual PWT – pretreatment average PWT/15.1 - pretreatment average PWT) × 100%.

2.7. Immunohistochemistry

At two weeks after surgery, rats (sham: n = 4; mSNI+: n = 6; mSNI−: n = 7) were euthanized using CO_2, immediately followed by transcardial perfusion with first approximately 100 ml of 0.1 M phosphate-buffered saline (PBS) and then 500 ml of 4% paraformaldehyde in 0.1 M PBS (PF). Spinal cords were post-fixed overnight in the same PF solution and then transferred to 10% sucrose in 0.1 M PBS for 24 h incubation. After a further 72 h incubation in 25% sucrose in 0.1 M PBS, the lumbar spinal cords were rapidly frozen using powdered dry ice and then stored at −80 °C until cryosectioning. The L4 and L5 spinal cord were embedded in Tissue-Tek (O.C.T., Sakura FineTek) and then transversally cut (30 μm-thickness), collecting every 12th section on Superfrost® Plus object glass slides (Thermo Scientific, Gerhard Menzel GmbH, Germany). Glass slides with transversal tissue sections were stored at −80 °C until immunohistological staining. Two immunostainings were performed in this investigation, targeting the microglial marker; ionized calcium binding adaptor molecule 1 (Iba1) and the astrocytic marker; glial fibrillary acidic protein (GFAP). Glass slides were thawed for about half an hour at room temperature and then washed three times with PBS. For Iba1 staining, sections were incubated for 1 h in PBS containing 1% Triton X-100 and 5% normal goat serum (NGS), followed by an overnight incubation in primary antibody solution at 4 °C (α-Iba1; WAKO, cat. no. 019/19741; 1:1000 in PBS-T containing 1% NGS). For GFAP staining, sections were immediately incubated overnight in primary antibody solution at 4 °C (α-GFAP; DAKO, cat. no. IS524; 1:1000 in PBS-T). Then next day, sections were incubated in secondary antibody solution for 1 h at room temperature; goat *anti*-rabbit Alexa-594 (Invitrogen, Belgium), diluted 1:100 in PBS and 1% Triton X-100 (for Iba1 staining this solution also contained 1% NGS). At the end of this incubation, glass slides were again washed three times with PBS and then coverslipped using 80% glycerol in PBS.

2.8. Image analysis

The immuno-stained sections were examined under a digital inverted EVOS microscope (Advanced Microscopy Group, Mill Creek, Washington) that uses a light-emitting diode (LED) illumination system and was equipped with a Texas Red light cube. At 4× magnification, photomicrographs were taken from the L4 spinal cord. A total of 5 photomicrographs per animal were used for image analysis. Photomicrographs were then loaded into *NIH* Image J analysis software (version 1.47) and background signals were subtracted. Then, the complete dorsal horn was selected as the region of interest (ROI) according to the rat atlas of Paxinos and Watson. The area-percentage within this ROI showing immunoreactivity (IR) for Iba1 or GFAP was determined. The percentages measured for each of the five photomicrographs were then averaged per animal and expressed relative to sham-operated rats. The analysis was performed by three independent investigators (J.D., N.D., B.Ba.), blinded for the experimental conditions.

2.9. Statistics

Data are reported as mean ± standard error (SE) values. Algesimetric data were analysed statistically using the log-values of the PWT. In order to test for differences between baseline PWT and 7-day PWT, paired student's t-tests were performed. Non-paired student's t-tests were performed to compare the day-1 SSI score of mSNI + and mSNI − rats as well as the MPE of CCG63802-treated rats and MPE of vehicle-treated rats at individual timepoints. qRT-PCR and immunohistochemical data of sham-operated, mSNI + and mSNI − animals were compared using a one-way analysis of variance (ANOVA) with a Dunnett post hoc correction (considering sham-operated rats as reference group). A two-way ANOVA with Bonferroni posthoc correction was used to compare SSI scores over time for mSNI + and mSNI − animals. Statistics and preparation of graphs was done using GraphPad Prism version 5.03 (GraphPad Software, San Diego, CA; www.graphpad.com). A p-value of 0.05 was regarded as the level of statistical significance.

3. Results

3.1. Clamp crush completely and specifically abolishes conduction along injured nerve branches

An ex vivo approach was used to determine whether the impact of the lesion procedure was restricted to the injured branches. Here, sciatic nerve samples were acutely isolated from adult rats and electrophysiological experiments were performed before and after crushing of the tibial and common peroneal, but not sural nerve branches (Fig. 1A, B). Before injury, responses from the three peripheral nerve branches increased gradually with augmenting pulse strengths (Fig. 1C, left). After injury, responses from the two crushed branches were completely abolished and remained absent throughout the observational period of up to 5.5 h (Fig. 1C, right), explaining a full lack of peak conduction velocities that had been recorded from these branches prior to crush (Fig. 1D). In contrast, conduction along the spared sural nerve remained unaffected after crush of the tibial and common peroneal branches (Fig. 1E). On the basis of this data we concluded that the crush procedure was suitable to induce lesions restricted to the injured branches of the sciatic nerve.

3.2. Restricting crush to the common peroneal nerve branch reduces prevalence of tactile hypersensitivity

Development of tactile hypersensitivity is a typical and consistent feature of rodent models of peripheral nerve injury. We here aimed to investigate whether the extent of tissue trauma in models of peripheral nerve injury influences the development of tactile hypersensitivity. For this purpose, we used the classical model of SNI in which two peripheral branches of the sciatic nerve are injured (Decosterd and Woolf, 2000) and compared tactile sensitivity at one week following surgery with that of a modified version of the SNI model (mSNI) in which the injury was restricted to only a single peripheral branch of the sciatic nerve, i.e. the common peroneal branch. The PWT at baseline was consistent for all animals, with values around the cut-off of 15.1 g. At one week after surgery, nearly all SNI animals had PWT values well below the baseline (Fig. 2A), while this was not the case for mSNI animals in which values were either around or below baseline (Fig. 2B). Sham-operated animals showed nearly identical PWT values before and one week after surgery (data not shown). mSNI animals were then subdivided based on a 7-day

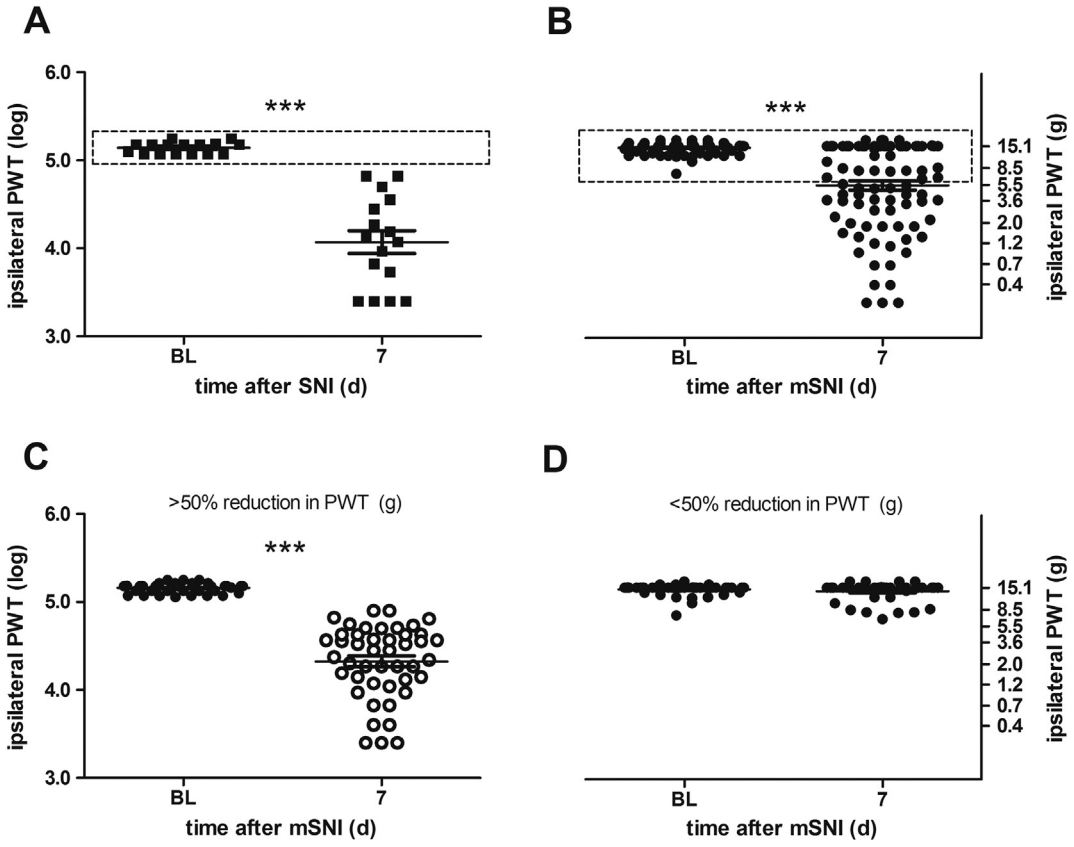

Fig. 2. Distinct outcomes for tactile sensitivity at one week after classical or modified spared nerve injury. A, B; PWT are shown before and after crush injury to either the common peroneal branch and tibial branch (SNI, n = 21, A) or the common peroneal branch only (mSNI, n = 103, B). The dashed boxes indicate the spread of individual PWT at BL. Note that all individual 7-days post-injury PWT are below those of BL for SNI, but not mSNI. Data of 103 mSNI rats were then clustered in two groups, i.e. one group in which the 7-days post-injury PWT (in grams) was 50% lower than at BL (C; n = 50) and one group where this difference did not exceed 50% (D; n = 53). *PWT*, paw withdrawal threshold; *g*, grams; *BL*, baseline; *(m)SNI*; (modified) spared nerve injury; *d*, days; ***, $p < 0.001$ (BL vs. 7-days post-injury).

PWT that was reduced by more or <50% of the individual baseline PWT value, respectively. While the former category was found to have a statistically significant reduction in PWT, the latter category did not show any statistically significant reduction (Fig. 2C–D). The mSNI animals with and without statistically significant reduction in PWT were designated mSNI+ and mSNI−, respectively. On the basis of a total number of 103 rats that underwent mSNI surgery, the ratio of mSNI+/mSNI− was 0.49/0.51.

3.3. Development of tactile hypersensitivity after mSNI shows no relation with the extent of motor deficits or recovery

The remarkable divergence in the presence or absence of tactile hypersensitivity after mSNI surgery made us wonder whether other lesion outcomes were affected by subgroup category. mSNI surgery was performed on 15 rats and these were followed daily for the static sciatic index (SSI), a sciatic nerve-dependent motor read-out (Bervar, 2000). Compared to baseline, animals in the mSNI+ and mSNI− group showed a similar drop in SSI score at one day after surgery (Fig. 3A). Likewise, the recovery of SSI scores that occurred spontaneously over the course of 2–3 weeks, was unaffected by subgroup category (Fig. 3B).

3.4. Role of RGS4 in tactile hypersensitivity at one week after mSNI

A divergence between development and absence of tactile hypersensitivity after nerve lesion has been previously linked to the functionality of inhibitory systems in the nociceptive neuraxis (De Felice et al., 2011) and we and others have implicated the spinal RGS4 in disinhibition processes after nerve lesion (Bosier et al., 2015; Garnier et al., 2003). Therefore, a putative role of RGS4 in tactile hypersensitivity following mSNI was explored here. Gene expression of RGS4 was found to be statistically significantly elevated in both the lumbar dorsal root ganglia and dorsal spinal cord, ipsilaterally, but not contralaterally to the nerve lesion in mSNI+ animals as compared to sham controls (Fig. 4A–D). mSNI− animals did not show such an elevation in gene expression. The possibility of an a-specific up-regulation of RGS members in mSNI+ animals was unlikely as RGS2 gene expression was also evaluated and not found to be regulated by either nerve lesion or subgroup category (Fig. 4E–H). As these data suggested an involvement of RGS4 in the onset of tactile hypersensitivity after mSNI, we designed an interference experiment using the specific RGS4 inhibitor CCG63802 as used previously (Bosier et al., 2015). This inhibitor was dissolved in vehicle solution (5% DMSO in saline) and administered intrathecally at 7 days after surgery to mSNI+ animals, after which tactile sensitivity was monitored every 20 min for a total duration of 2 h. Control mSNI+ animals underwent the same procedure with the exception that the intrathecal injection comprised 5% DMSO in saline without the RGS4 inhibitor CCG63802. mSNI+ animals treated with the inhibitor showed a rapid, but transient reduction in tactile hypersensitivity (Fig. 5). At 20 min, the effect was 59 ± 11% of what was maximally possible, and this was further increased to 70 ± 7% after 40 min. At 1 h after injection the effect was reduced to 29 ± 8% of the maximum-possible-effect (i.e. size of the effect in reference of control values) and hereafter PWT returned to pre-treatment hypersensitivity values. Saline treatment did not affect PWT at any time point within the 2 h-observation period (Fig. 5).

3.5. Persistence of tactile hypersensitivity at two weeks after mSNI and link with central gliosis

Clinical studies have proposed that early tactile hypersensitivity after surgery may be linked to persistent pain (Lavand'homme et al., 2005; Martinez et al., 2012). We therefore wanted to explore the persistence of tactile hypersensitivity in our model of mSNI. PWT were determined at two weeks after surgery for animals that were categorized as mSNI+ and mSNI− at one week after surgery. We found that 26 out of 33 animals (i.e. 79%) remained within the mSNI+ category, while this was the case for 28 out of 33 animals (i.e. 85%) within the mSNI− category (Fig. 6A). In a cohort of 15 animals that was followed for 4 weeks, the percentages of mSNI+ and mSNI− rats, which remained in the same category throughout the 4 week observation period were 84% and 89%, respectively (data not shown).

The persistence of pain hypersensitivity after nerve injury has been strongly linked to processes of gliosis within the CNS. Particularly, microglial reactivity and astrocytosis in the dorsal horn of the lumbar spinal cord have been implicated in chronic pain-like behaviours of models in which the sciatic nerve is injured (Ji et al., 2006; Tsuda et al., 2005). We therefore selected animals that showed consistence in mSNI+ or mSNI− at two weeks after surgery and performed an immunohistochemical analysis of microglial Iba1 and astrocytic GFAP expression in the ipsilateral lumbar dorsal horn and compared this with that of sham-operated control animals. We found a statistically significant up-regulation for both glial markers in mSNI+ animals, but not mSNI− animals, as compared to sham-operated controls (Fig. 6B, C). Representative images of the immunostained sections for both animal groups are shown in Fig. 7.

4. Discussion

In this manuscript we report on a new model of peripheral nerve injury in the rat in which the restriction of nerve trauma from two to a single injured branch of the sciatic nerve reduces the prevalence of tactile hypersensitivity. With this model we revealed a role of injury-induced RGS4 expression in the development of tactile hypersensitivity, while motor deficits seemed to be unrelated to RGS4, occurring to the same extent in animals with and without up-regulated RGS4. Finally, the presence or absence of tactile hypersensitivity was found to be mostly

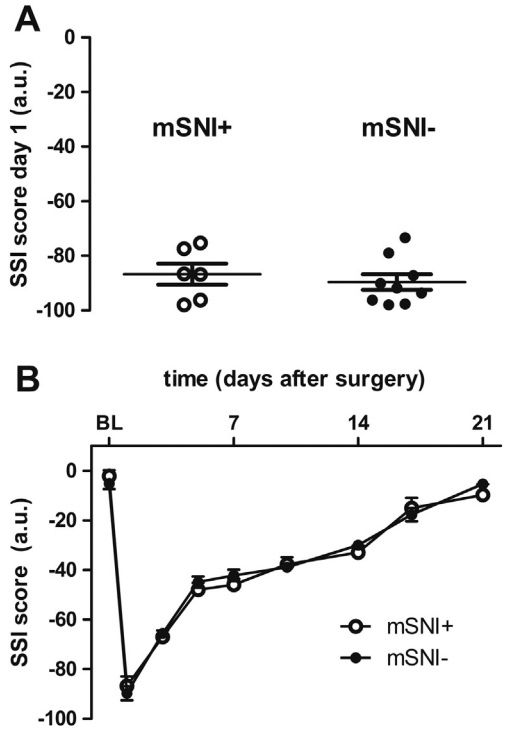

Fig. 3. Deficit and recovery of sciatic nerve-dependent motor function is similar between mSNI rats with and without tactile hypersensitivity. A; SSI scores at one day after mSNI+ (n = 6) and mSNI− (n = 9) animals. Note that the category 'mSNI+' and 'mSNI−' was determined at 7 days after nerve injury. B; evolution of SSI scores over the course of three weeks after mSNI surgery. *SSI*, static sciatic index; a.u.; arbitrary units; *mSNI+*; *d*, days; modified spared nerve injury with tactile hypersensitivity at 7 days after surgery; *mSNI−*; modified spared nerve injury without tactile hypersensitivity at 7 days after surgery.

persistent for at least another week, and could be associated with neuro-immune processes involving glial cells in the dorsal horn of the lumbar spinal cord.

Great advances have been made in our understanding of the mechanisms that underlie pain in the early phases after surgical insults such as nerve lesions (Berger et al., 2011; Ren and Dubner, 2010; Scholz and Woolf, 2007). The mechanisms of pain at later stages are also increasingly being explored (Ji et al., 2013; Milligan and Watkins, 2009), highlighting alterations in immune-related markers in chronic pain conditions (Marchand et al., 2005; Uceyler et al., 2007; Uceyler et al., 2010). In strong contrast, we only know little about what mediates the transition from acute to chronic pain or about what protects against

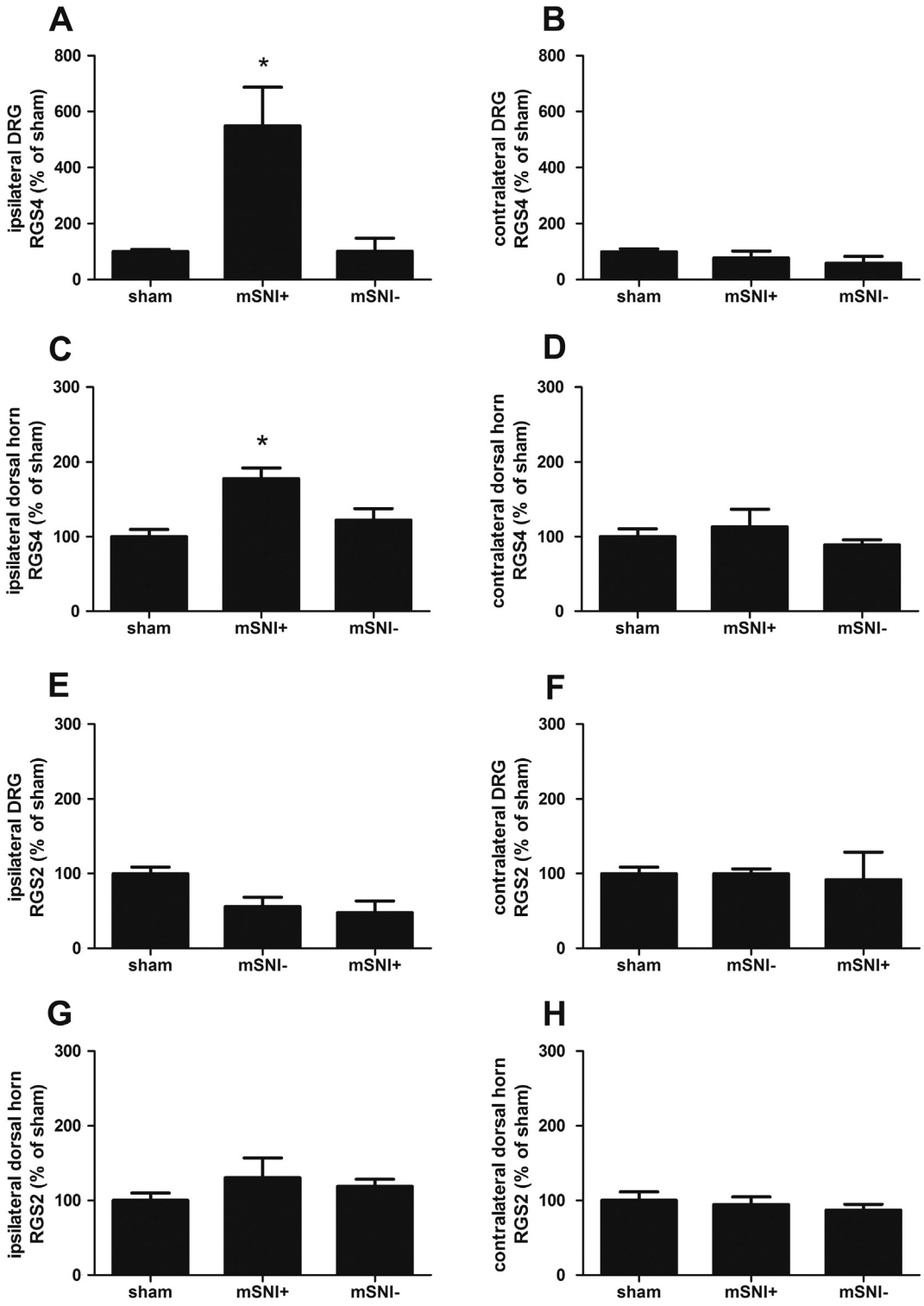

Fig. 4. RGS4 and RGS2 expression in lumbar DRGs and dorsal spinal cord at 7 days after mSNI. Animals were subdivided into mSNI+ (n = 5) and mSNI− (n = 8) at 7 days after mSNI surgery and qRT-PCR for RGS4 and RGS2 was performed on lumbar (L4 and L5) DRGs ipsilateral (A, E) and contralateral (B, F) to the surgery with sham-operated (n = 4) animals serving as controls. The same was done for the ipsilateral and contralateral lumbar dorsal cords (C, D, G, H respectively). *DRG*, dorsal root ganglia; *RGS*, Regulator of G protein Signaling; *mSNI+*; modified spared nerve injury with tactile hypersensitivity at 7 days after surgery; *mSNI−*; modified spared nerve injury without tactile hypersensitivity at 7 days after surgery; *, $p < 0.05$ (vs. sham).

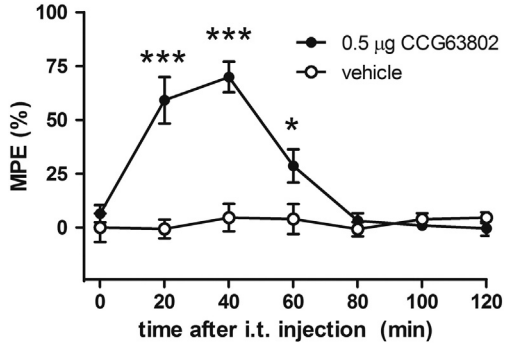

Fig. 5. Spinal RGS4 inhibition transiently reverses tactile hypersensitivity in mSNI + rats. A bolus injection of the RGS4 inhibitor CCG63802 or vehicle solution (5% DMSO) was given to mSNI + rats at 7 days after surgery. The PWT was determined every 20 min for a total duration of 2 h and results were expressed as MPE for CCG63802 (n = 6) and vehicle-treated rats (n = 5). *MPE*, maximum possible effect; *DMSO*; dimethyl sulfoxide; *i.t.*, intrathecal; *min*, minutes; *** and *, $p < 0.001$ and $p < 0.05$, respectively (CCG63802 vs. vehicle treatment).

the development of chronic pain states (Katz and Seltzer, 2009; Voscopoulos and Lema, 2010). Since tactile hypersensitivity in the early postoperative phase has been clinically implicated in the chronification of pain (Deumens et al., 2013) and tactile hypersensitivity is considered one of the most debilitating symptoms of neuropathic pain syndromes (Bennett, 1994), we here focused on this symptom. Previous work has shown that the genetic background of rodents (De Felice et al., 2011; Yoon et al., 1999), but also the amount of spared neural tissue (Kloos et al., 2005) can influence the prevalence of tactile hypersensitivity after neurotrauma. By reducing the extent of trauma to the sciatic nerve we could observe a reduction in the prevalence of tactile hypersensitivity in the present study. Nevertheless, the presence or absence of tactile hypersensitivity within the mSNI model seemed not to be caused by differential extents of tissue trauma for several reasons. First, the selected lesion procedure was robust and has been validated previously (Luis et al., 2007). Second, our electrophysiological data showed that the lesion procedure rendered a complete disappearance of signal conduction along injured fibers, but left it fully intact in spared nerve fibers. Third, the SSI, which is a reliable read-out for sciatic nerve function (Bervar, 2000) showed an identical drop and recovery for mSNI animals with and without tactile hypersensitivity.

In order to better understand this divergent pain-related outcome after mSNI, we decided to explore a possible role of RGS4. We recently reported RGS4 as a negative regulator of signaling through the analgesic CB_1 receptor, reducing its activity in the spinal cord ipsilateral to a partial sciatic nerve ligation (Bosier et al., 2015). This suggested that the up-regulation of RGS4 could be part of a nerve injury-evoked mechanism that causes disinhibition in the dorsal horn of the spinal cord. A divergence between disinhibition and engagement of inhibitory systems has indeed been previously linked to the presence and absence of tactile hypersensitivity after nerve injury (De Felice et al., 2011). Our current data showed that an up-regulation of RGS4 occurred in the lumbar DRGs and dorsal horns of only nerve lesioned animals that showed tactile hypersensitivity. Blocking of RGS4 through the intrathecal delivery of a specific inhibitor attenuated tactile hypersensitivity, an effect that was seen from 20 min after drug administration, but did not outlast the first hour. The transient nature of this effect may explain why, in previous work, we could not observe an effect of spinal RGS4 inhibition on tactile hypersensitivity when the interval between drug delivery and algesimetric testing reached several hours (Bosier et al., 2015).

Over the past years, members of the RGS family have been increasingly linked with nociception and analgesia (Han et al., 2010; Ibi et al., 2011; Psifogeorgou et al., 2011; Zachariou et al., 2003). More recent data also suggested a role of RGS in pathological pain states (Terzi et al., 2014; Yoon et al., 2015) (Mitsi et al., 2015; Salaga et al., 2016), which is further strengthened by the data on RGS4 in our current paper. Nevertheless, many unresolved issues remain such as 'what is the identity of the cells expressing RGS4?' The lack of suitable antibodies for immunohistochemical investigations limits advances in this direction, but the RGS-pain story may be further complicated by factors such as the lesion model. For example, sciatic nerve transection has been reported to reduce the number of primary sensory DRG neurons expressing RGS3 or RGS4 transcripts (Costigan et al., 2003) as opposed to an up-regulation of RGS4 transcripts in the DRG and spinal cord following partial sciatic nerve ligation and mSNI ((Bosier et al., 2015; Garnier et al., 2003) and data in the current study). Also the signaling events that are up-stream and down-stream of an RGS4 up-regulation after nerve injury remain unknown. While RGS proteins have been implicated in many different cellular functions (Hollinger and Hepler, 2002), RGS4 is just a small member of the family containing little

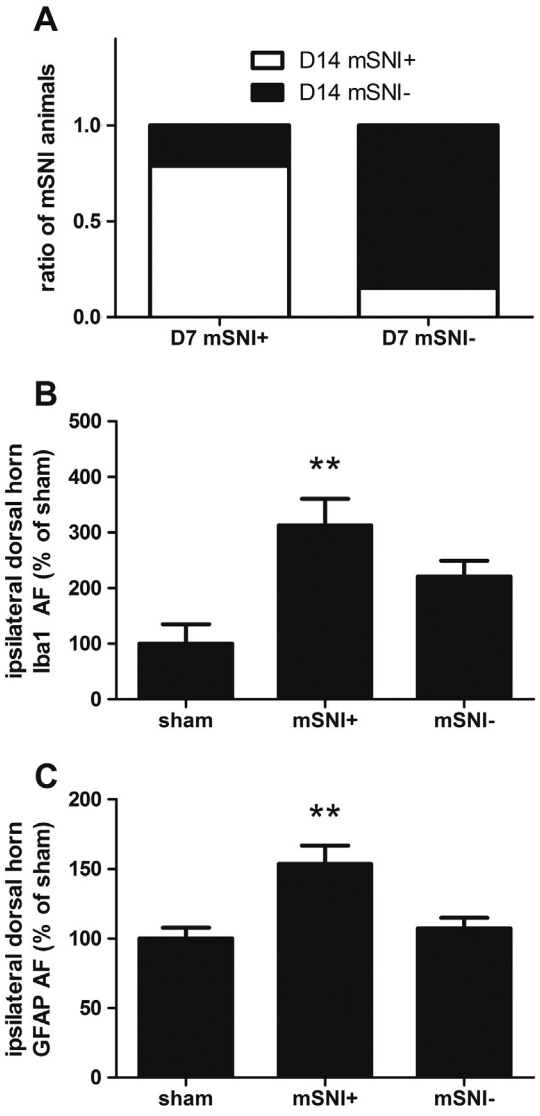

Fig. 6. Tactile sensitivity outcomes and glial reactivity in the lumbar dorsal horn at 14 days after mSNI. A, using the criterium of 50% decrease from BL-PWT values, rats were subdivided into mSNI + and mSNI − animals, both at 7 and 14 days after mSNI. Note in the stacked bars that the vast majority of mSNI + and mSNI − animals at 7 days remain in their respective category at 14 days. Microglial and astrocytic reactions of mSNI + (n = 6) and mSNI − (n = 7) rats with consistent outcomes were determined on the basis of immunohistochemical analysis, using sham-operated rats as controls (n = 4). The area fraction of the ipsilateral lumbar (L4-5) dorsal horn that was immunoreactive for either the microglial marker Iba1 or the astrocytic marker GFAP was determined. *Iba1*; ionized-calcium binding adapter molecule-1; *GFAP*, glial fibrillary acidic protein; *AF*, area fraction; *mSNI +*; modified spared nerve injury with tactile hypersensitivity at 7 days after surgery; *mSNI −*; modified spared nerve injury without tactile hypersensitivity at 7 days after surgery; **, $p < 0.01$ (vs. sham).

more than a single RGS domain that may relate to its full functionality. We and others have shown that RGS4 negatively influences the signaling through G protein-coupled receptors that are known for having analgesic effects, such as the CB_1 and μ-opioid receptors (Bosier et al., 2015; Garnier et al., 2003). Whether such action may explain the tactile hypersensitivity in 50% of mSNI animals remains to be investigated, but preliminary data already suggested no effect of mSNI surgery on the signaling efficacy through CB_1 receptors (data not shown). Even though the exact mechanisms by which RGS4 inhibition caused a reversal of tactile hypersensitivity remain unknown for now, data from the literature leads us to assume that specific targeting of the spinal cord was important for the observed effect. Indeed, systemic depletion of RGS4 fully preserved tactile hypersensitivity after SNI in mice (Stratinaki et al., 2013). This may be explained by an RGS4 action in supraspinal sites that opposes the therapeutic effect of spinal RGS4 inhibition. In support of this, depletion of RGS4 in the nucleus accumbens was found to reduce the analgesic effect of opiate analgesics (Han et al., 2010). While challenging in a clinical setting, a spinal targeting of RGS4 inhibition may be beneficial also for limiting unwanted side effects. In support of this, our data showed a specific association of RGS4 up-regulation with tactile hypersensitivity, but not sciatic nerve-dependent motor function, as assessed with the SSI. Also, previous work showed no motor impairments after intrathecal treatment with the same RGS4 inhibitor used in the current investigation (Bosier et al., 2015).

A great advantage of the mSNI model could lie in the possibility to distinguish between pathobiological alterations that specifically relate to the development of hypersensitivity as opposed to other injury-related symptoms and events. For now, an up-regulation of RGS4 appears to be part of a hypersensitivity-specific signature in the total of neurochemical alterations that follow peripheral nerve injury. Whether the model of mSNI will be a further asset in the search of pain chronification mechanisms remains to be determined in future investigations. While it is interesting to note that the vast majority of rats showing tactile hypersensitivity at one week after mSNI, retained this symptom for at least three more weeks, our study did not focus on persistence of pain states, which can be rather heterogeneous and reach well beyond tactile hypersensitivity (Dworkin, 2002). Notably, however, we did observe a higher glial reactivity in the dorsal horns of animals showing tactile hypersensitivity than in those without this pain-like behaviour. Microglia and astrocytes have been both heavily implicated in the inception and maintenance of neuropathic pain (Aldskogius and Kozlova, 2013; Ji et al., 2006; Tsuda et al., 2005) and chronic pain has even been considered as a possible result of 'diseased glia' (Ji et al., 2013). Then again, care should be taken with any conclusions in this direction, as injury-induced glial reactivity is not necessarily linked with painful outcomes (Gallo et al., 2015; Leinders et al., 2013). Many 'activation' states may exist, only some of which are 'pain-related' (McMahon and Malcangio, 2009). We speculate that the mSNI model with its divergent outcomes on tactile hypersensitivity, could help to distinguish between pain-related and non-pain-related activation states. The latter are even more interesting in light of recent work showing that microglial cells are not required for tactile hypersensitivity in female rats, as opposed to male rats (Sorge et al., 2015). In our investigation we exclusively used female rats as women seem to suffer from chronic

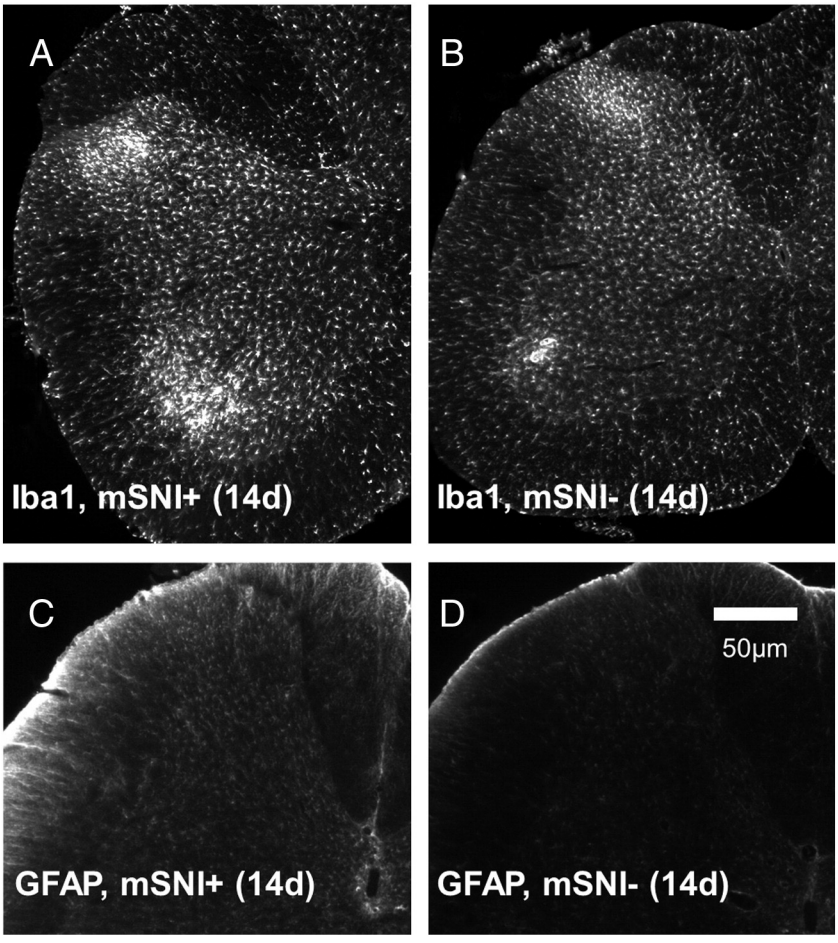

Fig. 7. Representative Iba1 and GFAP immunostainings of the L4 dorsal horn in mSNI + and mSNI − rats. Photomicrographs represent a section at the L4 spinal cord level, encompassing the full dorsal horn ipsilateral to mSNI, which was performed 14 days earlier. Iba1 immunoreactivity is shown for mSNI + (A) and mSNI − (B) rats; GFAP is shown for mSNI + (C) and mSNI − (D) rats as well. The scale bar in D applies to panels A-D. *Iba1*; ionized-calcium binding adapter molecule-1; *GFAP*, glial fibrillary acidic protein *mSNI +*; modified spared nerve injury with tactile hypersensitivity at 7 and 14 days after surgery; *mSNI −*; modified spared nerve injury without tactile hypersensitivity at 7 and 14 days after surgery.

pain disorders more than men (Berkley, 1997; Grosu and de Kock, 2011). As pathological pain mechanisms (including those following nerve lesion) may fundamentally differ between the two genders (Sorge et al., 2011), it remains to be seen whether the mSNI model with divergent tactile sensitivity outcomes applies to the male gender as well.

In summary, a multitude of animal models of peripheral nerve injury have been developed over the course of the last decades (Gregory et al., 2013). While the specific set of neuropathic pain-like behaviours, either spontaneous or evoked by thermal, tactile or chemical stimuli, may differ from model to model, a feature that is generally shared among models is the consistency in pain behaviours, such as tactile hypersensitivity. Since only a fraction of surgical patients develops tactile hypersensitivity (Lavand'homme et al., 2005; Martinez et al., 2012), current animal models with persistent tactile hypersensitivity may have strong limitations when trying to understand what happens in the early postoperative phase that may drive an acute postoperative pain to either spontaneous resolution or transition into a chronic pain problem. We here report on a new rat model of nerve injury in which only the common peroneal branch of the sciatic nerve is injured leading to an approximate 50% prevalence of tactile hypersensitivity. With this model we could, for now, demonstrate that RGS4 was specifically associated with the development of tactile hypersensitivity.

Acknowledgements

The authors declare no competing financial interests. Pr Stefano Geuna (University of Turin, Italy) is warmheartedly thanked for lending us the nerve clamp. This work was financially supported by the Fonds de la Recherche Scientifique (F.R.S. - FNRS). B.Bo. and G.T. received funding from F.R.S. - FNRS; R.D. was funded by the UCL (FSR Incoming fellowship) and F.R.S.-FNRS.

References

Aldskogius, H., Kozlova, E.N., 2013. Microglia and neuropathic pain. CNS & Neurological Disorders Drug Targets 12, 768–772.
Baron, R., Binder, A., Wasner, G., 2010. Neuropathic pain: diagnosis, pathophysiological mechanisms, and treatment. The Lancet Neurology 9, 807–819.
Bennett, G., 1994. Neuropathic pain. In: P.D., W., Melzack, R. (Eds.), Textbook on Pain, 3rd edn, pp. 201–224.
Berger, J.V., Knaepen, L., Janssen, S.P., Jaken, R.J., Marcus, M.A., Joosten, E.A., Deumens, R., 2011. Cellular and molecular insights into neuropathy-induced pain hypersensitivity for mechanism-based treatment approaches. Brain Res. Rev. 67, 282–310.
Berkley, K.J., 1997. Sex differences in pain. The Behavioral and Brain Sciences 20, 371–380 (discussion 435–513).
Bervar, M., 2000. Video analysis of standing–an alternative footprint analysis to assess functional loss following injury to the rat sciatic nerve. J. Neurosci. Methods 102, 109–116.
Blom, S.M., Pfister, J.P., Santello, M., Senn, W., Nevian, T., 2014. Nerve injury-induced neuropathic pain causes disinhibition of the anterior cingulate cortex. J. Neurosci. 34, 5754–5764.
Bosier, B., Doyen, P.J., Brolet, A., Muccioli, G.G., Ahmed, E., Desmet, N., Hermans, E., Deumens, R., 2015. Inhibition of the regulator of G protein signalling RGS4 in the spinal cord decreases neuropathic hyperalgesia and restores cannabinoid CB1 receptor signalling. Br. J. Pharmacol. 172, 5333–5346.
Bouhassira, D., Lanteri-Minet, M., Attal, N., Laurent, B., Touboul, C., 2008. Prevalence of chronic pain with neuropathic characteristics in the general population. Pain 136, 380–387.
Chaplan, S.R., Bach, F.W., Pogrel, J.W., Chung, J.M., Yaksh, T.L., 1994. Quantitative assessment of tactile allodynia in the rat paw. J. Neurosci. Methods 53, 55–63.
Costigan, M., Samad, T.A., Allchorne, A., Lanoue, C., Tate, S., Woolf, C.J., 2003. High basal expression and injury-induced down regulation of two regulator of G-protein signaling transcripts, RGS3 and RGS4 in primary sensory neurons. Mol. Cell. Neurosci. 24, 106–116.
De Felice, M., Sanoja, R., Wang, R., Vera-Portocarrero, L., Oyarzo, J., King, T., Ossipov, M.H., Vanderah, T.W., Lai, J., Dussor, G.O., Fields, H.L., Price, T.J., Porreca, F., 2011. Engagement of descending inhibition from the rostral ventromedial medulla protects against chronic neuropathic pain. Pain 152, 2701–2709.
Decosterd, I., Woolf, C.J., 2000. Spared nerve injury: an animal model of persistent peripheral neuropathic pain. Pain 87, 149–158.
Deumens, R., Steyaert, A., Forget, P., Schubert, M., Lavand'homme, P., Hermans, E., De Kock, M., 2013. Prevention of chronic postoperative pain: cellular, molecular, and clinical insights for mechanism-based treatment approaches. Prog. Neurobiol. 104, 1–37.
Dworkin, R.H., 2002. An overview of neuropathic pain: syndromes, symptoms, signs, and several mechanisms. Clin. J. Pain 18, 343–349.
Gallo, A., Dimiziani, A., Damblon, J., Michot, B., Des Rieux, A., De Kock, M., Hermans, E., Deumens, R., 2015. Modulation of spinal glial reactivity by intrathecal PPF is not sufficient to inhibit mechanical allodynia induced by nerve crush. Neurosci. Res. 95, 78–82.
Garnier, M., Zaratin, P.F., Ficalora, G., Valente, M., Fontanella, L., Rhee, M.H., Blumer, K.J., Scheideler, M.A., 2003. Up-regulation of regulator of G protein signaling 4 expression in a model of neuropathic pain and insensitivity to morphine. J. Pharmacol. Exp. Ther. 304, 1299–1306.
Gregory, N.S., Harris, A.L., Robinson, C.R., Dougherty, P.M., Fuchs, P.N., Sluka, K.A., 2013. An overview of animal models of pain: disease models and outcome measures. The Journal of Pain: Official Journal of the American Pain Society 14, 1255–1269.
Grosu, I., de Kock, M., 2011. New concepts in acute pain management: strategies to prevent chronic postsurgical pain, opioid-induced hyperalgesia, and outcome measures. Anesthesiol. Clin. 29, 311–327.
Han, M.H., Renthal, W., Ring, R.H., Rahman, Z., Psifogeorgou, K., Howland, D., Birnbaum, S., Young, K., Neve, R., Nestler, E.J., Zachariou, V., 2010. Brain region specific actions of regulator of G protein signaling 4 oppose morphine reward and dependence but promote analgesia. Biol. Psychiatry 67, 761–769.
Hollinger, S., Hepler, J.R., 2002. Cellular regulation of RGS proteins: modulators and integrators of G protein signaling. Pharmacol. Rev. 54, 527–559.
Ibi, M., Matsuno, K., Matsumoto, M., Sasaki, M., Nakagawa, T., Katsuyama, M., Iwata, K., Zhang, J., Kaneko, S., Yabe-Nishimura, C., 2011. Involvement of NOX1/NADPH oxidase in morphine-induced analgesia and tolerance. J. Neurosci. 31, 18094–18103.
Ji, R.R., Berta, T., Nedergaard, M., 2013. Glia and pain: is chronic pain a gliopathy? Pain 154 (Suppl 1), S10–S28.
Ji, R.R., Kawasaki, Y., Zhuang, Z.Y., Wen, Y.R., Decosterd, I., 2006. Possible role of spinal astrocytes in maintaining chronic pain sensitization: review of current evidence with focus on bFGF/JNK pathway. Neuron Glia Biol. 2, 259–269.
Katz, J., Seltzer, Z., 2009. Transition from acute to chronic postsurgical pain: risk factors and protective factors. Expert. Rev. Neurother. 9, 723–744.
Kehlet, H., Jensen, T.S., Woolf, C.J., 2006. Persistent postsurgical pain: risk factors and prevention. Lancet 367, 1618–1625.
Kloos, A.D., Fisher, L.C., Detloff, M.R., Hassenzahl, D.L., Basso, D.M., 2005. Stepwise motor and all-or-none sensory recovery is associated with nonlinear sparing after incremental spinal cord injury in rats. Exp. Neurol. 191, 251–265.
Lavand'homme, P., 2011. The progression from acute to chronic pain. Curr. Opin. Anaesthesiol. 24, 545–550.
Lavand'homme, P., De Kock, M., Waterloos, H., 2005. Intraoperative epidural analgesia combined with ketamine provides effective preventive analgesia in patients undergoing major digestive surgery. Anesthesiology 103, 813–820.
Leinders, M., Knaepen, L., De Kock, M., Sommer, C., Hermans, E., Deumens, R., 2013. Up-regulation of spinal microglial Iba-1 expression persists after resolution of neuropathic pain hypersensitivity. Neurosci. Lett. 554, 146–150.
Luis, A.L., Amado, S., Geuna, S., Rodrigues, J.M., Simoes, M.J., Santos, J.D., Fregnan, F., Raimondo, S., Veloso, A.P., Ferreira, A.J., Armada-da-Silva, P.A., Varejao, A.S., Mauricio, A.C., 2007. Long-term functional and morphological assessment of a standardized rat sciatic nerve crush injury with a non-serrated clamp. J. Neurosci. Methods 163, 92–104.
Marchand, F., Perretti, M., McMahon, S.B., 2005. Role of the immune system in chronic pain. Nat. Rev. Neurosci. 6, 521–532.
Martinez, V., Ben Ammar, S., Judet, T., Bouhassira, D., Chauvin, M., Fletcher, D., 2012. Risk factors predictive of chronic postsurgical neuropathic pain: the value of the iliac crest bone harvest model. Pain 153, 1478–1483.
McMahon, S.B., Malcangio, M., 2009. Current challenges in glia-pain biology. Neuron 64, 46–54.
Milligan, E.D., Watkins, L.R., 2009. Pathological and protective roles of glia in chronic pain. Nat. Rev. Neurosci. 10, 23–36.
Mitsi, V., Terzi, D., Purushothaman, I., Manouras, L., Gaspari, S., Neve, R.L., Stratinaki, M., Feng, J., Shen, L., Zachariou, V., 2015. RGS9-2—controlled adaptations in the striatum determine the onset of action and efficacy of antidepressants in neuropathic pain states. Proc. Natl. Acad. Sci. U. S. A. 112, E5088–E5097.
Psifogeorgou, K., Terzi, D., Papachatzaki, M.M., Varidaki, A., Ferguson, D., Gold, S.J., Zachariou, V., 2011. A unique role of RGS9-2 in the striatum as a positive or negative regulator of opiate analgesia. J. Neurosci. 31, 5617–5624.
Ren, K., Dubner, R., 2010. Interactions between the immune and nervous systems in pain. Nat. Med. 16, 1267–1276.
Salaga, M., Storr, M., Martemyanov, K.A., Fichna, J., 2016. RGS proteins as targets in the treatment of intestinal inflammation and visceral pain: new insights and future perspectives. BioEssays: News and Reviews in Molecular, Cellular and Developmental Biology 38, 344–354.
Scholz, J., Woolf, C.J., 2007. The neuropathic pain triad: neurons, immune cells and glia. Nat. Neurosci. 10, 1361–1368.
Smits, H., Ultenius, C., Deumens, R., Koopmans, G.C., Honig, W.M., van Kleef, M., Linderoth, B., Joosten, E.A., 2006. Effect of spinal cord stimulation in an animal model of neuropathic pain relates to degree of tactile "allodynia". Neuroscience 143, 541–546.
Sorge, R.E., LaCroix-Fralish, M.L., Tuttle, A.H., Sotocinal, S.G., Austin, J.S., Ritchie, J., Chanda, M.L., Graham, A.C., Topham, L., Beggs, S., Salter, M.W., Mogil, J.S., 2011. Spinal cord Toll-like receptor 4 mediates inflammatory and neuropathic hypersensitivity in male but not female mice. J. Neurosci. 31, 15450–15454.
Sorge, R.E., Mapplebeck, J.C., Rosen, S., Beggs, S., Taves, S., Alexander, J.K., Martin, L.J., Austin, J.S., Sotocinal, S.G., Chen, D., Yang, M., Shi, X.Q., Huang, H., Pillon, N.J., Bilan, P.J., Tu, Y., Klip, A., Ji, R.R., Zhang, J., Salter, M.W., Mogil, J.S., 2015. Different immune cells mediate mechanical pain hypersensitivity in male and female mice. Nat. Neurosci. 18, 1081–1083.

Stratinaki, M., Varidaki, A., Mitsi, V., Ghose, S., Magida, J., Dias, C., Russo, S.J., Vialou, V., Caldarone, B.J., Tamminga, C.A., Nestler, E.J., Zachariou, V., 2013. Regulator of G protein signaling 4 [corrected] is a crucial modulator of antidepressant drug action in depression and neuropathic pain models. Proc. Natl. Acad. Sci. U. S. A. 110, 8254–8259.

Terzi, D., Gaspari, S., Manouras, L., Descalzi, G., Mitsi, V., Zachariou, V., 2014. RGS9-2 modulates sensory and mood related symptoms of neuropathic pain. Neurobiol. Learn. Mem. 115, 43–48.

Torrance, N., Smith, B.H., Bennett, M.I., Lee, A.J., 2006. The epidemiology of chronic pain of predominantly neuropathic origin. Results from a general population survey. The Journal of Pain: Official Journal of the American Pain Society 7, 281–289.

Tsuda, M., Inoue, K., Salter, M.W., 2005. Neuropathic pain and spinal microglia: a big problem from molecules in "small" glia. Trends Neurosci. 28, 101–107.

Uceyler, N., Eberle, T., Rolke, R., Birklein, F., Sommer, C., 2007. Differential expression patterns of cytokines in complex regional pain syndrome. Pain 132, 195–205.

Uceyler, N., Kafke, W., Riediger, N., He, L., Necula, G., Toyka, K.V., Sommer, C., 2010. Elevated proinflammatory cytokine expression in affected skin in small fiber neuropathy. Neurology 74, 1806–1813.

von Hehn, C.A., Baron, R., Woolf, C.J., 2012. Deconstructing the neuropathic pain phenotype to reveal neural mechanisms. Neuron 73, 638–652.

Voscopoulos, C., Lema, M., 2010. When does acute pain become chronic? Br. J. Anaesth. 105 (Suppl 1), i69–i85.

Yoon, Y.W., Lee, D.H., Lee, B.H., Chung, K., Chung, J.M., 1999. Different strains and substrains of rats show different levels of neuropathic pain behaviors. Exp. Brain Res. 129, 167–171.

Yoon, S.Y., Woo, J., Park, J.O., Choi, E.J., Shin, H.S., Roh, D.H., Kim, K.S., 2015. Intrathecal RGS4 inhibitor, CCG50014, reduces nociceptive responses and enhances opioid-mediated analgesic effects in the mouse formalin test. Anesth. Analg. 120, 671–677.

Zachariou, V., Georgescu, D., Sanchez, N., Rahman, Z., DiLeone, R., Berton, O., Neve, R.L., Sim-Selley, L.J., Selley, D.E., Gold, S.J., Nestler, E.J., 2003. Essential role for RGS9 in opiate action. Proc. Natl. Acad. Sci. U. S. A. 100, 13656–13661.